CHEMISTRY LETTERS, pp. 2223-2226, 1992.

Scanning Surface Potential Microscopy for Local Surface Analysis

Masamichi FUJIHIRA,* Hirosuke KAWATE, and Masatoshi YASUTAKE+
Department of Biomolecular Engineering, Tokyo Institute of Technology,
4259 Nagatsuta, Midori-ku, Yokohama 227
+Seiko Instruments Inc., Scientific Instruments Division, Development Department,
563, Takatsuka-shinden, Matsudo, Chiba 271

A Scanning Surface Potential Microscopic (SSPM) instrument was built by modifying a commercial atomic force microscope (AFM), Seiko SFA 300 with a SPI 3600 probe station. Distribution of surface potentials on test samples micro-lithographically prepared and on mixed Langmuir-Blodgett (LB) films coated on a vapor-deposited gold film could be imaged in a x-y spatial resolution less than 1 μm and compared with AFM images observed on the same samples.

Since the invention of the scanning tunneling microscope (STM),[1] other scanning probe microscopes (SPM) such as an atomic force microscope (AFM)[2] have been devised to image surfaces from the micron scale down to the atomic scale. Many studies have already demonstrated that the STM and AFM can effectively image organic thin films and surfaces.[3] However, these methods are rather insensitive to chemical compositions. Recently, we succeeded in demonstrating that a friction force microscope (FFM)[4-8] can detect the difference between domains composed of unlike chemical species.[3,9]

Although friction is highly material dependent, another kind of SPM which is sensitive to surface chemical properties is also desired. Among several candidates, high-resolution potentiometry by electrostatic force microscopy is most promising, because the voltage measurements on a p-n junction[10] or on a commercial operational amplifier[11] with submicron spatial resolution were demonstrated already. From macroscopic measurements it is well known that surface potentials or contact potential differences are highly material dependent and are related to work functions and surface dipole moments.[12] Recently, Yokoyama et al. applied the method to measure the localized surface potential distribution on test samples consisting of aluminum islands of micron sizes deposited on platinum surface or on LB films of phospholipids and of photosensitive dye molecules.[13] They named the method the scanning Maxwell stress microscopy (SMM).

In the present work, we built our own SSPM (i.e. SMM) by modifying a commercial AFM and demonstrate that the SSPM can detect the surface potentials on test samples prepared microlithographically and on the phase-separated domains in the mixed monolayers.

Figure 1 shows the schematic diagram of the present SSPM which is based on the design by Yokoyama et al.[13] The electrostatic force on a conducting tip held close to a conducting surface is given by

$$F = -(1/2)V^2(\partial C/\partial z) \quad (1)$$

where V denotes the potential difference between sample surface and tip.[11,13] If the tip potential is sinusoidally driven by an external source so as to give $V = V_{DC} + V_{AC} \sin(\omega t)$, there appear three force components, i.e. DC, ω-, and 2ω-components, each of which gives information on the electrostatic properties of the surface and the surrounding medium. The amplitude of vibration of the tip A will be given by

$$A = S \times [V_{DC}^2 + 2V_{DC}V_{AC} \sin(\omega t) + (V_{AC}^2 / 2)(1 - \cos(2\omega t))] \qquad (2)$$

where S is the (ill defined) calibration factor relating potential difference to amplitude of vibration and includes the elastic response of the tip as well as $(\partial C / \partial z)$. The surface potential difference V_{DC} can be obtained from the ω-component, and the effective tip-surface separation from the 2ω-component.

A test sample consisting of vapor-deposited gold stripes on a chromium film on a glass plate was kindly given by Micro Products Research Laboratory, Dai Nippon Printing Co., Saitama. Another test sample was prepared by gold vapor deposition coating on microlithographically prepared numeral patterns with a height of ca. 100 nm. The mixed monolayer[3,9] of perfluorodecanoic acid (Asahi Glass Co.) and arachidic acid (Tokyo Kasei Organic Chemicals) was spread on the aqueous subphase containing 0.04 mM poly(4-methylvinyl-pyridinium) iodide[14] and then transferred at 40 mN m^{-1} on a vapor-deposited gold film on a glass plate with a Langmuir trough equipped with an electronic microbalance and a glass Wilhelmy plate (Kyowa Kaimen Kagaku Co., HMB-AP).

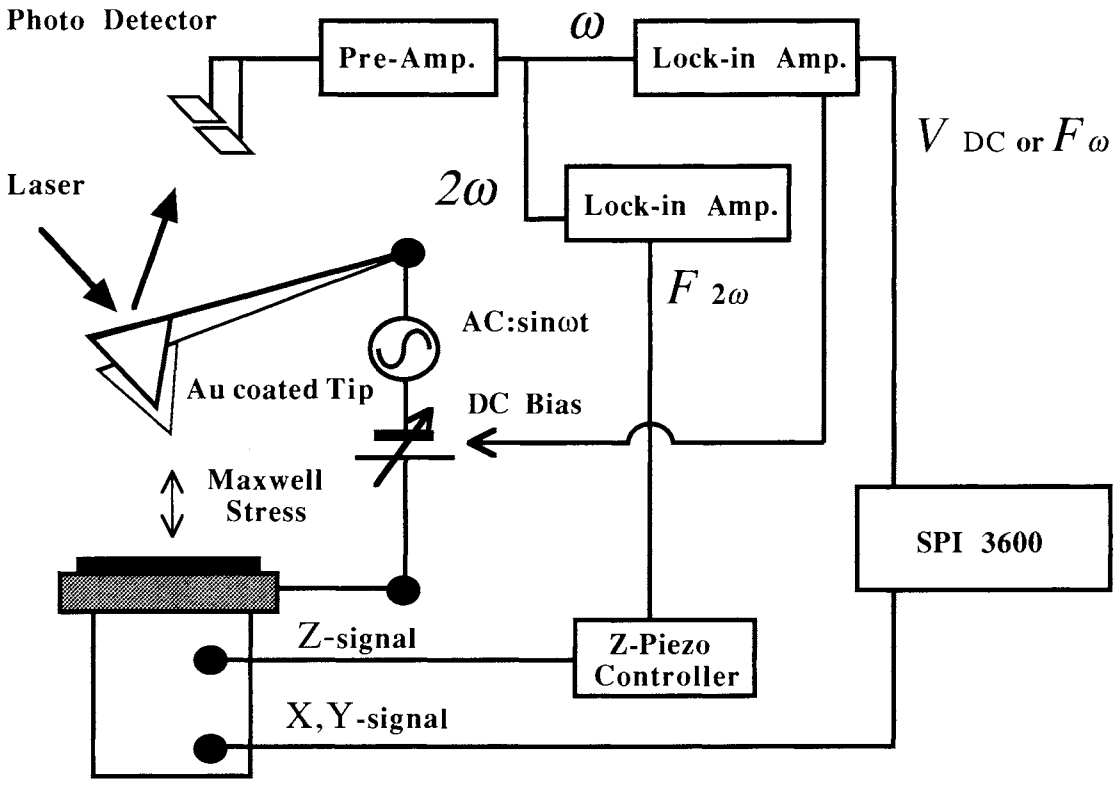

Fig. 1. The schematic diagram of a scanning surface potential microscope.

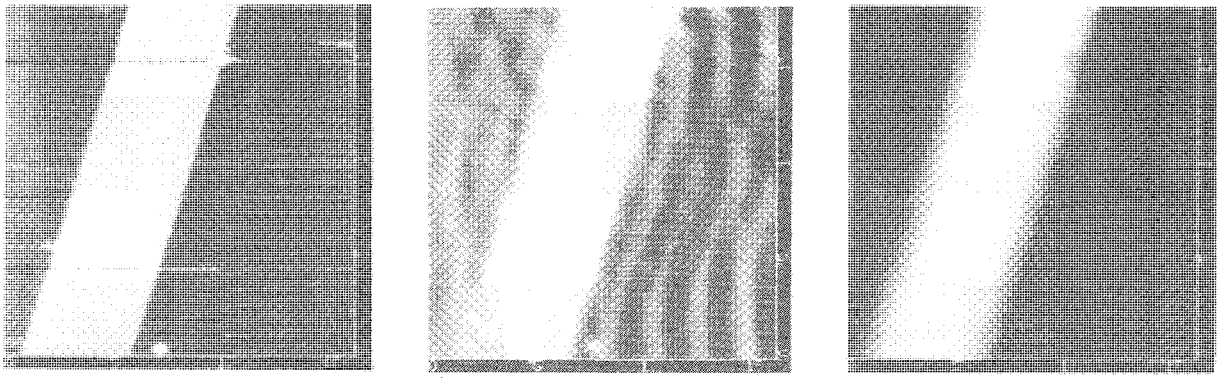

Fig. 2. AFM (a), topography of SMM (b), and SSPM (c) images of a Au stripe on a Cr film.

Figure 2a shows a 15.0 x 15.0 μm^2 top view AFM image of the test sample consisting of gold stripes on a chromium film. The gold stripe (ca. 5 μm in width and ca. 43 nm in height) above the chromium flat film was observed. As shown in Fig. 2b, the similar topographic top view image of SMM, but with much higher noise level, was obtained by the constant capacitance mode, i.e. by keeping the amplitude of the 2ω-component constant. When the change in the amplitude of the ω-component was displayed in a x-y frame, this gave us a top view SSPM image of the test sample as shown in Fig. 2c. The observed change in the surface potentials between the gold stripe and the chromium base film was attributed to the difference in work functions between gold and chromium.[15] The faded color observed on the border between the gold and chromium surfaces in the SSPM image in contrast with the drastic change in color in the corresponding region of the AFM image clearly indicates that the spatial resolution of SSPM is much less than that of AFM. However, the resolution was improved effectively together with an increase in the contrast of the image by placing the tip closer to the sample surface, i.e. by increasing the amplitude of 2ω-component not due to V_{AC} but due to the increase in S in Eq. 1.

On the other numeral test sample which has only a gold surface with two different heights of 100 nm difference, the similar SMM topographic image was observed in the constant capacitance mode, but negligibly weak contrast was observed in the SSPM image as we would expect for the sample coated only with one kind of metal, i.e. gold.

Figure 3a shows a 15.0 x 15.0 μm^2 top view AFM image of a vapor-deposited gold film surface on a glass plate covered with a polyion complexed mixed monolayer of $C_9F_{19}COOH$ and $C_{19}H_{39}COOH$. But the image was almost the same as an AFM image observed for the same gold surface uncovered with the mixed monolayer. This indicates that the surface roughness of the gold surface was too large to see the topography of the mixed monolayer itself. The difference in heights between the hydrocarbon islands and the fluorocarbon sea is clearly seen in an AFM image for the same mixed monolayer deposited on a hydrophilic silicon (100) surface as shown in Fig. 3b. The image was similar to those previously observed for a mixed monolayer of arachidic acid with a different type of fluorinated amphiphile.[3,9] Figure 3c shows a top view of a SSPM image observed on the same surface for the AFM image of Fig. 3a. In spite of the roughness of the surface as shown in Fig. 3a, an image with clear contrast of the surface potential difference between the hydrocarbon islands and the fluorocarbon sea is discernible. From the comparison between the images of Figs. 3b and 3c, it is clearly shown that even the islands smaller than 1 μm in diameter can be seen in the SSPM image. The surface potential

difference between the islands and the sea is attributable to the difference in the surface dipole moments due to the terminal CH_3- and CF_3- groups.[16] The macroscopic surface potential difference between the pure polyion complexed monolayers of $C_9F_{19}COOH$ and $C_{19}H_{39}COOH$ deposited on the same gold films was measured to be ca. 0.5 V.

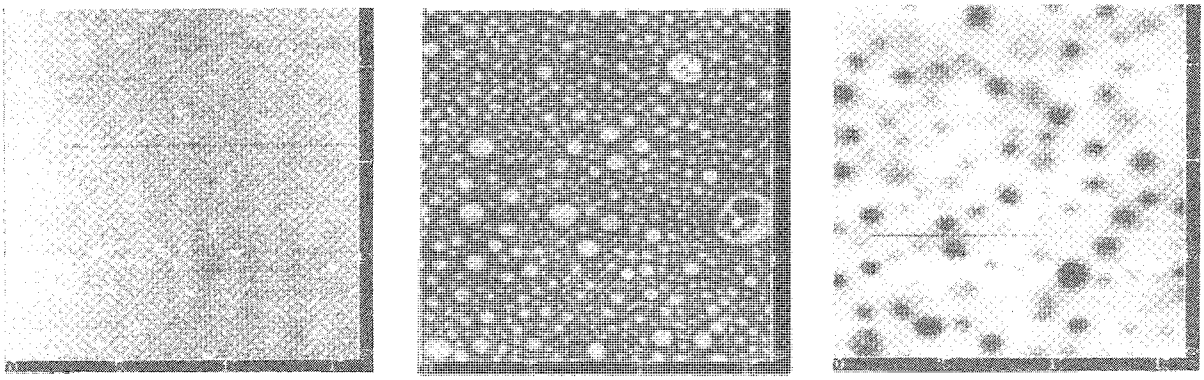

(a) (b) (c)

Fig. 3. AFM (a) and SSPM (c) images of a Au film covered with a polyion complexed mixed monolayer of $C_9F_{19}COOH$ and $C_{19}H_{39}COOH$ (1:1) and AFM (b) image of the same mixed monolayer on Si (100).

This work was supported by a Grant-in Aid for Scientific Research on Priority Areas (New Functionality Materials) and on New Program (03NP0301) from the Ministry of Education, Science, and Culture of Japan.

References

1) G. Binnig, H. Rohrer, C. Gerber, and E. Weibel, *Appl. Phys. Lett.*, **40**, 178 (1982).
2) G. Binnig, C. F. Quate, and C. Gerber, *Phys. Rev. Lett.*, **56**, 930 (1986).
3) J. Frommer, *Angew. Chem.*, in press.
4) C. M. Mate, G. M. McClelland, R. Erlandsson, and S. Chiang, *Phys. Rev. Lett.*, **59**, 1942 (1987).
5) G. Meyer and N. M. Amer, *Appl. Phys. Lett.*, **57**, 2089 (1990).
6) O. Marti, J. Colchero, and J. Mlynek, *J. Nanotechnology*, **1**, 141 (1990).
7) R. Erlandsson, S. Chiang, G. M. McClelland, C. M. Mate, and G. Hadziiannou, *J. Chem. Phys.*, **89**, 5190 (1988).
8) E. Meyer, L. Howald, R. Overney, D. Brodbeck, R. Lüthi, H. Haefke, J. Frommer, and H.-J. Güntherodt, *Ultramicroscopy*, in press.
9) E. Meyer, R. Overney, R. Lüthi, D. Brodbeck, L. Howald, J. Frommer, H.-J. Güntherodt, O. Wolter, M. Fujihira, H. Takano, and Y. Gotoh, *Thin Solid Films*, in press; R. M. Overney, E. Meyer, J. Frommer, D. Brodbeck, R. Lüthi, L. Howald, H.-J. Güntherodt, M. Fujihira, H. Takano, and Y. Gotoh, *Nature*, **359**, 133 (1992).
10) Y. Martin, D. W. Abraham, and H. K. Wickramasinghe, *Appl. Phys. Lett.*, **52**, 1103 (1988).
11) J. M. R. Weaver and D. W. Abraham, *J. Vac. Sci. Technol.*, **B9**, 1559 (1991).
12) G. L. Gaines, Jr.,"Insoluble Monolayers at Liquid-Gas Interfaces," John Wiley, New York (1966).
13) H. Yokoyama, K. Saito, and T. Inoue, *Mol. Electronics. Bioelectronics*, **3**, 79 (1992).
14) J. Umemura, Y. Hishiro, T. Kawai, T. Takenaka, Y. Gotoh, and M. Fujihira, *Thin Solid Films*, **178**, 281 (1989).
15) J. O'M. Bockris and A. K. N. Reddy, "Modern Electrochemistry," Plenum, New York (1970), p.944.
16) V. Vogel and D. Möbius, *J. Colloid Interface Sci.*, **126**, 408 (1988).

(Received August 4, 1992)